Chinese Journal of
POLYMER SCIENCE

RESEARCH ARTICLE

https://doi.org/10.1007/s10118-022-2657-9
Chinese J. Polym. Sci. **2022**, *40*, 166–174

UV-Vis-NIR Light-deformable Shape-memory Polyurethane Doped with Liquid-crystal Mixture and GO towards Biomimetic Applications

Peng Zhang[a], Feng Cai[b], Guo-Jie Wang[a*], and Hai-Feng Yu[b*]

[a] *School of Materials Science and Engineering, University of Science and Technology Beijing, Beijing 100083, China*
[b] *Institute of New Structural Materials, School of Materials Science and Engineering, and Key Laboratory of Polymer Chemistry and Physics of Ministry of Education, Peking University, Beijing 100871, China*

Electronic Supplementary Information

Abstract Nature has been inspiring material researchers to fabricate biomimetic functional devices for various applications, and shape-memory polymer materials (SMPMs) have received tremendous attention since the promising intelligent materials possess more advantages over others for the fabrication of biomimetic functional devices. As is well-known, SMPMs can be stimulated by heat, electricity, magnetism, pH, solvent and light. From the viewpoint of practical applications, ultraviolet (UV)-visible (Vis)-near infrared (NIR) light-responsive SMPMs are undoubtedly more advantageous. However, up to now, UV-Vis-NIR light-deformable SMPMs by combining photothermal and photochemical effects are still rarely reported. Here we designed a UV-Vis-NIR light-deformable SMP composite film *via* incorporating a liquid crystal (LC) mixture and graphene oxide (GO) into a shape-memory polyurethane matrix. The elongated composite films exhibited interesting photomechanical bending deformations with different light-triggered mechanisms, (1) photochemically induced LC phase transition upon UV exposure, (2) photochemically and photothermally induced LC phase transition upon visible-light irradiation, (3) photothermally triggered LC phase transition and partial stress relaxation upon low-intensity NIR exposure. All the deformed objects could recover to their original shapes by high-intensity NIR irradiation. Moreover, the biomimetic circadian rhythms of acacia leaves and the biomimetic bending/spreading of fingers were successfully achieved, which could blaze a way in the field of biomimetic functional devices due to the excellent light-deformable and shape-memory properties of the SMP composite films.

Keywords UV-Vis-NIR; Light-deformable; Shape-memory; Liquid-crystal; Biomimetic functional device

Citation: Zhang, P.; Cai, F.; Wang, G. J.; Yu, H. F. UV-Vis-NIR light-deformable shape-memory polyurethane doped with liquid-crystal mixture and GO towards biomimetic applications. *Chinese J. Polym. Sci.* **2022**, *40*, 166–174.

INTRODUCTION

The variety of movements in the biological world has provided inspirations to material scientists and engineers for the engineering of biomimetic functional devices. Among various potential materials capable of utilization for biomimetic functional systems, polymer materials possess incomparable advantages over others due to their light weight, suppleness, low costs, and more importantly, high processability and easy functionalization.[1] Shape-memory polymer (SMP) is a prominent class of smart materials that can be deformed when programmed above their shape-memory transition temperatures which can be a glass transition temperature, a melting temperature or less commonly liquid crystal clearing temperature,[2] allowing remoulding and recycling processes.[3,4] Due to their superior properties, SMP materials (SMPMs) have been applied to the fields of soft actuators and functional devices.[5] Currently, the most widely investigated SMPMs are thermally,[6–9] electrically,[10,11] magnetically,[12,13] pH[14] and humidity[15] responsive, *etc*. However, the traditional stimuli (such as heat, electricity, magnetism, *etc*.) usually require the external energy input. On the other hand, light can be used as a precise stimulus, which can be controlled remotely and rapidly.[16–19] Light-deformable SMPMs can directly convert light energy into mechanical energy upon light irradiation, which seem to be promising in miniaturized functional devices.

As is well-known, azobenzene has been used as a molecular switch to convert light energy into the conformational change,[20,21] which subsequently enables the materials macroscopically deformable upon ultraviolet (UV) exposure.[22–26] Therefore, incorporation of azobenzene chromophores into SMPMs can endow them with photoresponse.[27,28] Nevertheless, UV light is non-ideal for practical applications because it can accelerate the aging and fading of materials, and bring great harmfulness to organisms.[29] In comparison, the long-wavelength visible (Vis) or near-infrared (NIR) light can penetrate into deeper tissues and bring less damage to materials or organisms.[30] Currently, two strategies may be adopted to endow azobenzene-containing SMPMs with multi-

* Corresponding authors, E-mail: guojie.wang@mater.ustb.edu.cn (G.J.W.)
E-mail: yuhaifeng@pku.edu.cn (H.F.Y.)

Received August 25, 2021; Accepted October 20, 2021; Published online January 1, 2022

© Chinese Chemical Society
Institute of Chemistry, Chinese Academy of Sciences

wavelength light response: (a) modification of azobenzene structures, which usually requires the structural design and tedious synthesis, (b) introduction of up-conversion materials (UCMs), which is dissatisfactory due to the high cost, complex synthesis and low up-conversion efficiency of UCMs. In our previous work,[31] UV-Vis-NIR light-deformable poly (vinyl alcohol) (PVA) composites were fabricated by doping with an azobenzene-containing liquid crystal (LC) mixture and graphene oxide (GO), however, they were short of the recyclable shape reprogramming capability owning to the inability to reprogram the deformations. Developing the materials that allow for shape re-moulding would greatly increase the potential of light-responsive materials, alleviating the present restrictions in actuation design and freedom, and SMPMs can be repeatedly moulded when heated above their shape-memory temperatures, enabling them attractive as highly versatile materials for light-driven functional devices. Therefore, we prepared UV-Vis-NIR light-deformable SMPMs doped with azobenzene and UCM,[32] which could be re-deformed and recycled. However, the green light-induced *trans*-to-*cis* isomerization degree of azobenzene was so small that the bending speeds of the composite films were slower upon green light exposure. In addition, the up-conversion efficiency of the UCM was lower, so the NIR light intensity and exposure time had to be significantly increased to gain large deformations of the composite films. Besides, all the deformations of the composite films returned to their original shapes only by heating rather than irradiating.

Here, to solve the above-mentioned problems, we presented a composite with rapid UV-Vis-NIR light-deformations and shape reprogramming, in which a commercially available shape-memory polyurethane (SMPU) served as the matrix, giving the material remoulding and recycling properties, an azobenzene-containing LC mixture and GO acted as the phase transition component and photothermal conversion component, respectively. The elongated composite films showed fast and large photomechanical bending deformations upon UV/Vis/NIR exposure, and all the deformations of the composite films could recover to their original shapes by high-intensity NIR irradiation. By utilization of the light-deformable shape-memory composite films (SMCFs), the biomimetic circadian rhythms of acacia leaves and the biomimetic bending/spreading of fingers were successfully achieved. The UV-Vis-NIR light-deformable composite film has paved the way towards biomimetic functional devices due to its good wavelength selectivity, fast and large light-deformations and excellent shape-memory properties, which will be practically applicable as sunlight-driven functional materials in the near future.

EXPERIMENTAL

Materials

P-aminobenzonitrile (Beijing Norway Technology, Beijing, China; 98%), hydrochloric acid (Xilong Science, Beijing, China; 36 wt%–38 wt%), sodium acetate (CH_3COONa, Xilong Science, Beijing, China; 99%), potassium carbonate (K_2CO_3, Xilong Science, Beijing, China; 99%), Sodium nitrite ($NaNO_2$, Xilong Chemical, Zhengzhou, China; 99%), Phenol (Sinopharm Chemical Reagent, Beijing, China; 99%), *n*-pentyl bromide (Sinopharm Chemical Reagent, Beijing, China; 99%), potassium iodide (KI, Sinopharm Chemical Reagent, Beijing, China; 99%), Ammonia solution (Beijing Chemical Plant, Beijing, China; 25 wt%), 4-cyano-4′-pentyl biphenyl (5CB, Sinopharm Chemical Reagent, Beijing, China; 98%), SMPU solution (Haina Environmental Protection Technology, Jining, China; 35 wt%), GO (Sinopharm Chemical Reagent, Beijing, China; 98%) were used as received.

Synthesis of 4-Cyano-4′-pentyloxyazobenzene

The azobenzene compound 4-cyano-4′-pentyloxyazobenzene (5CAZ) was synthesized by referring to the previously reported literature.[32]

Preparation of Azobenzene-containing LC Mixtures

In this section, the LC mixture with 5 mol% 5CAZ was taken as an example. Firstly, 5CAZ (7.4 mg, 0.025 mmol) and 5CB (0.12 g, 0.48 mmol) were dissolved in 0.4 mL of THF. After evaporation of the solvent, the LC mixture in liquid state was obtained. Other LC mixtures with different molar fractions of 5CAZ were prepared by the similar steps.

Preparation of SMPU-based Composite Films

In this section, the 5CAZ/5CB/GO/SMPU film with 3 wt‰ GO was taken as an example. As shown in Scheme S1 (in the electronic supplementary information, ESI), firstly, 11 mg of GO was ultrasonically dispersed in 1.2 mL of DMF. Then 9.6 g of SMPU solution containing 3.4 g of SMPU and 0.23 g of LC mixture with 5 mol% 5CAZ were added to the former dispersion system, and the mixture was stirred at 80 °C for 5 h. After cooling to room temperature, the resulting solution was uniformly cast on the glass substrate and dried at 80 °C for 12 h. Finally, the 5CAZ/5CB/GO/SMPU film with a thickness of about 0.3 mm was obtained by peeling off the glass substrate. Other composite films with different component contents were prepared by the similar steps. The component contents of the composite films are shown in Table S1 (in ESI).

The elongated composite films were prepared as follows. The composite films with original dimensions of 10 mm (length) × 5 mm (width) × 0.3 mm (thickness) were stretched to 200% strains at 65 °C with a rate of 2 mm/min, and then the elongated shapes of the films were fixed at 65 °C for 12 h to release the residual stress, followed by cooling to room temperature slowly to obtain the elongated composite films.

Characterization

The morphology of the cross section of the composite film was observed by using a scanning electron microscope (SEM, SU8010, HITACHI). The LC texture of 5CAZ, the LC textures and light-induced phase transitions of the LC mixtures, and the optical anisotropy of the composite film were observed by using a polarizing optical microscope (POM, Axio Scope A1, ZEISS). The UV-visible absorption spectra of 5CAZ and the composite films were recorded using a UV/VIS/NIR spectrometer (Lambda 750, PerkinElmer). 365 nm UV and 460 nm blue lights were performed by using a controller (HTLD-4, Shenzhen Height-LED Photoelectric Technology Co., Ltd.), and 808 nm NIR light was performed using a controller (MDL-H, Changchun New Industries Photoelectric Technology Co., Ltd.). The light intensities of light sources were measured by a photometer (CEL-NP2000, Zhongjiao Jinyuan Technology Co., Ltd.). The surface temperatures of the LC mixtures and the composite

films were monitored by using an infrared imaging system (SC7000, FLIR).

The thermodynamic properties of 5CAZ, SMPU and the LC mixtures were measured by a differential scanning calorimeter (DSC, DSC 8000, PerkinElmer). The LC mixtures were heated from −20 °C to 60 °C at a rate of 10 °C/min, 5CAZ from −20 °C to 160 °C at a rate of 10 °C/min, and SMPU from −50 °C to 120 °C at a rate of 20 °C/min. All the samples were sealed in aluminium pans and measured in nitrogen atmosphere.

The dynamic mechanical analysis of SMPU was performed by using a rheometer (MCR 301, Anton Paar Physica) (Fig. S1 in ESI). SMPU was heated from −10 °C to 100 °C at a rate of 3 °C/min. The diameter of the parallel plate: 8 mm, the gap spacing: 0.3 mm, strain: 0.1%, frequency: 1 Hz.

The tensile stress-strain measurements of the composite films were carried out by a universal testing machine (CMT-10, Jinan Liangong Testing Technology Co., Ltd.). The original dimensions of the composite films are 10 mm (length) × 5 mm (width) × 0.3 mm (thickness), which were stretched to fracture at room temperature with a rate of 5 mm/min to obtain the stress-strain curves.

The composite film with dimensions of 10 mm (length) × 5 mm (width) × 0.3 mm (thickness) was stretched to 200% strain at 65 °C. Upon subsequent cooling to room temperature under the load, the composite film reached a strain ε_{load}. After removing the stress, the composite film reached a fixed strain ε. Subsequently, under a stress free condition, the elongated composite film was heated to reach a recovered strain ε_{rec}. The shape fixing ratio R_f and shape recovery ratio R_r can be calculated by using the following equations:[2]

$$R_f = \frac{\varepsilon}{\varepsilon_{load}} \times 100\% \quad (1)$$

$$R_r = \frac{\varepsilon - \varepsilon_{rec}}{\varepsilon} \times 100\% \quad (2)$$

RESULTS AND DISCUSSION

Characterization of Azobenzene-containing LC Mixtures

The LC mixtures are composed of 5CAZ and 5CB in different molar ratios. 5CAZ is a nematic LC with a melting point (mp) of 110.8 °C and the LC-to-isotropic (I) phase transition temperature (T_i) of 117.8 °C (Fig. S2 in ESI), which serves as a photoswitch and undergoes the *trans*-to-*cis* isomerization upon 365 nm UV or 460 nm visible-light exposure (Fig. S3 in ESI). Similarly, 5CB is also a nematic LC with a mp of 18.8 °C and a comparatively low T_i of 36.0 °C, which is utilized to prepare low-T_i LC mixtures with 5CAZ, thereby enabling the LC mixtures to easily undergo photochemically or photothermally induced phase transitions. 5CAZ and 5CB were dissolved in THF in different molar ratios, upon evaporation of the solvent, the LC mixtures were obtained, which exhibited nematic LC textures at room temperature (Fig. 1a). Fig. 1(b) shows the thermodynamic properties of the LC mixtures. As the molar fraction of 5CAZ increases from 0% to 5%, the mps of the LC mixtures decrease from 18.8 °C to 16.2 °C while the T_is increase from 36.0 °C to 39.5 °C. However, when the molar fraction of 5CAZ exceeds 5%, a part of 5CAZ solids could separate out of the mixtures (Fig. S4 in ESI). Here, the LC mixture with 5 mol% 5CAZ is utilized for the following studies.

Subsequently, the LC-to-I phase transition of the LC mixture with 5 mol% 5CAZ was investigated. Before light irradiation, the LC mixture exhibited a nematic schlieren texture. When exposed to light, the entire field of vision became dark upon UV irradiation (365 nm, 110 mW/cm^2) for 7 s or visible-light (460 nm, 110 mW/cm^2) irradiation for 36 s (Movies S1 and S2 in ESI), and the surface temperatures of the LC mixture were much lower than its T_i (39.5 °C) in the process of light exposure (Fig. S5 in ESI), indicating the occurrence of the photochemically induced LC-to-I phase transition caused by the *trans*-to-*cis* isomerization of 5CAZ. It is worth noting that the LC-to-I phase transition of the LC mixture did not occur upon NIR exposure (808 nm, 210 mW/cm^2) (Movie S3 in ESI) due to the NIR light inertness of 5CAZ and 5CB.

Characterization of SMPU-based Composite Films

The composite films were prepared by drop-coating the SMPU solution on the glass substrate (Scheme S1 in ESI), the component contents of which are shown in Table S1 (in ESI). The SMPU-based composite film consists of three components: (a) SMPU (M_n=1.2×10^5 g/mol, PDI=2.2),[32] which serves as the matrix due to its good film formation and superior mechanical properties,[33] its chemical structure is shown in Fig. 2(a), diphenylmethane moieties act as hard segments and

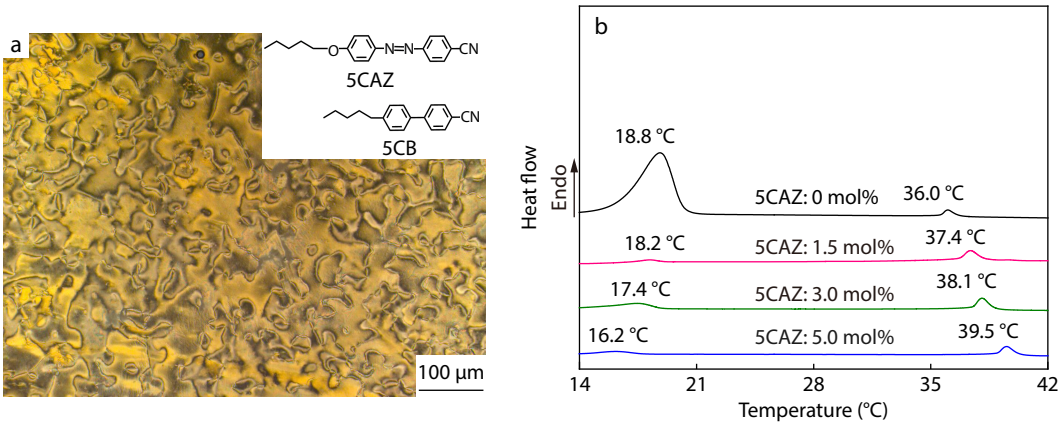

Fig. 1 (a) POM image of the LC texture of the LC mixture with 5 mol% 5CAZ. Inset: Molecular structures of 5CAZ and 5CB; (b) DSC curves of the LC mixtures.

https://doi.org/10.1007/s10118-022-2657-9

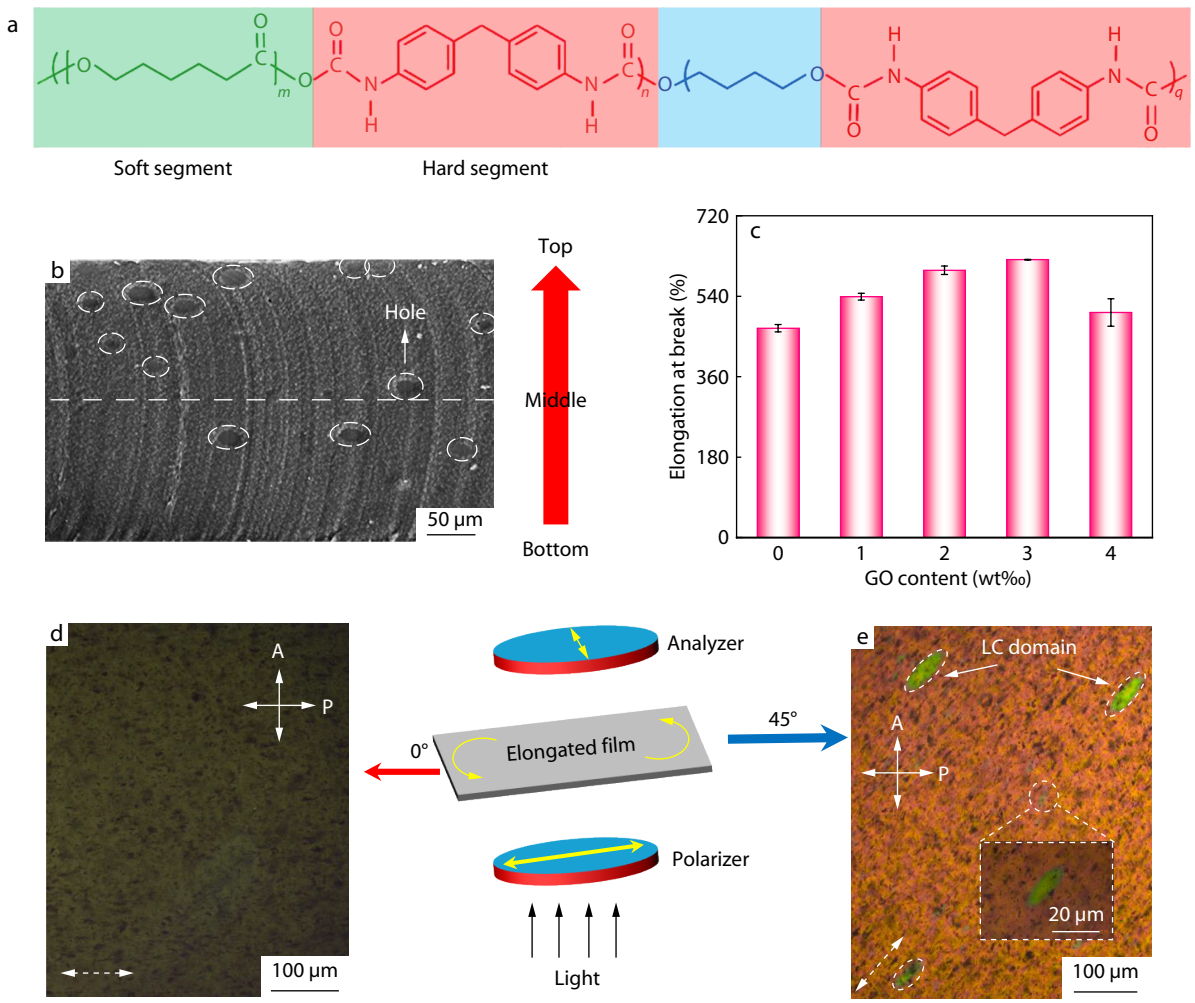

Fig. 2 (a) Chemical structure of SMPU; (b) SEM image of the cross section of the composite film after immersion in *n*-hexane for 24 h; (c) Changes in the EBs of the composite films with the mass fraction of GO; (d, e) POM images of the composite film with the stretching diecrtion parallel to each polarizer axe and at 45° to either of the polarizer axes, respectively. White solid arrows denote the axes of the polarizer (P) and analyzer (A), and white dashed ones represent the stretching direction of the film. Inset: enlarged POM image of the LC domain.

polycaprolactone moieties as soft segments,[34,35] its glass transition temperature of hard segments (T_gh) is 53.5 °C (Fig. S6 in ESI); (b) azobenzene-containing LC mixture, which acts as a photoswitch and undergoes the LC-to-I phase transition upon UV or visible-light exposure, and (c) GO, which possesses superior properties[36] and is utilized to convert the absorbed light energy into heat energy.

To determine the distribution of the LC mixture in the composite film, the film was immersed in *n*-hexane for 24 h, followed by drying at room temperature. Subsequently, the morphology of the cross section of the film was observed by SEM. Before immersion, the cross section of the composite film is imporous.[32,33] After immersion in *n*-hexane for 24 h, the cross section of the film is full of holes (Fig. 2b), indicating that the LC mixture has been successfully removed. Besides, Fig. 2(b) also shows that the number of holes in the upper part of the film is much more than that in the lower part, demonstrating that the composite film spontaneously forms a bilayer-like structure, the upper part of the film is a LC-rich layer and the lower part is a LC-poor one, which is because 5CAZ and 5CB with small surface energies tend to migrate to the upper surface to reduce the surface energy of the whole composite film.[32] Besides, the evaporation of DMF also contributes to the surface migrations of 5CAZ and 5CB due to their good solubility in DMF. In addition, to investigate the effect of GO on the mechanical properties of the composite films, five specimens with dimensions of 10 mm (length) × 5 mm (width) × 0.3 mm (thickness) were stretched by using a universal testing machine at room temperature with a rate of 5 mm/min. As shown in Fig. 2(c), with the increment of the mass fraction of GO, the elongations at break (EBs) of the composite films gradually increase due to the enhancement effect of GO,[33] whereas, when the mass fraction of GO exceeds 3‰, the EBs of the films significantly decrease probably because of the agglomeration of GO. Here, the composite film with 3 wt‰ GO, namely 5CAZ/5CB/GO(3wt‰)/SMPU, is utilized for the following studies.

Moreover, to enable the composite films light-deformable, the homogeneous orientation of LC domains is indispensable, while the mechanical stretching treatment is a relatively simple and effective approach to gaining the homogeneous orientation of LC domains along the stretching direc-

tion.[31–33] As expected, the lowest transmittance is observed when the stretching direction of the composite film is parallel to either of the polarizer axes (Fig. 2d), while the highest transmittance appears when the stretching direction of the film is at 45° to each polarizer axis (Fig. 2e), indicating the homogeneous orientation of LC domains along the stretching direction. Besides, as seen clearly from Fig. 2(e), the LC domains (green ellipsoids) in the composite film are indeed aligned along the stretching direction.

UV-Vis-NIR Light-induced Deformations

The light-deformable behaviors of 5CAZ/5CB/GO(3wt‰)/SMPU films were investigated upon UV/Vis/NIR exposure. As is well-known, volume contraction usually occurs upon transforming from the horizontally aligned LC phase to the isotropic phase, which can be utilized to induce the deformations of soft materials.[37] Although the volume contraction at microscopic scale is too weak to be detected, incorporating LC molecules into polymer matrixes may enhance the photomechanical effect.[38] That is to say, a small amount of LC molecules may bring about a macroscopical deformation. For the composite films, light can penetrate deep enough to trigger the LC-to-I phase transition.[32] Upon light irradiation, the horizontally aligned LC domains in the elongated composite films with bilayer-like structures underwent the LC-to-I phase transition, and then an asymmetric volume contraction occurred along the stretching direction. The elongated 5CAZ/5CB/GO(3wt‰)/SMPU films bent towards the UV/Vis/NIR light along the stretching direction when their top surfaces faced light sources (Movies S4–S6 in ESI), whereas, when the bottom surfaces of the elongated films were exposed to light, they bent away from the incident direction of the actinic light (Movies S7–S9 in ESI), which was because the upper part (LC-rich layer) of the composite film showed a larger volume contraction than the lower part (LC-poor layer) upon light exposure, similar to the so-called bimetal mechanism of LC elastomers.[39]

To quantitatively compare the deformation degrees of the composite films, a parameter of bending degree $F = (l_0 - l)/l_0$ is introduced, where l_0 and l are the linear lengths of the films before and after illumination, respectively.[31,32] Upon UV (365 nm, 110 mW/cm^2) exposure, the elongated SMPU and 5CB/SMPU films were nearly unbending while the elongated 5CAZ/5CB/SMPU film showed a large F value of 0.35 (Fig. 3a), indicating that 5CAZ was indispensable for the UV-induced bending deformation of the composite film. However, when GO was incorporated into the 5CAZ/5CB/SMPU film, the F value (F=0.32) of the elongated 5CAZ/5CB/GO(3wt‰)/SMPU film decreased slightly upon UV irradiation (Fig. 3a), which was because GO absorbed a part of UV light and enabled the decrease of the *trans*-to-*cis* photoisomerization degree of 5CAZ (Figs. S7a and S7b in ESI). In addition, in the process of UV irradiation, the surface temperatures of the elongated 5CAZ/5CB/SMPU and 5CAZ/5CB/GO(3wt‰)/SMPU films were always lower than the T_i (39.5 °C) of the LC mixture (Fig. 3b). The above results demonstrate that the UV-induced bending deformation of the elongated 5CAZ/5CB/GO(3wt‰)/SMPU film is mainly attributed to the photochemically triggered LC-to-I phase transition caused by the *trans*-to-*cis* photoisomerization of 5CAZ. Upon visible-light (460 nm, 110 mW/cm^2) irradiation, the elongated SMPU and 5CB/SMPU films were nearly unbending whereas the elongated 5CAZ/5CB/SMPU film showed a F value of 0.22 (Fig. 3c), and the surface temperature of the elongated 5CAZ/5CB/SMPU film was always much lower than the T_i (39.5 °C) of the LC mixture in the process of visible-light irradiation (Fig. 3d), indicating the photochemically induced bending deformation of the composite film triggered by the LC-to-I phase transition caused by the *trans*-to-*cis* photoisomerization of 5CAZ (Fig. S7c in ESI). When GO was introduced to the 5CAZ/5CB/SMPU film, the F value (F=0.31) of the elongated 5CAZ/5CB/GO(3wt‰)/SMPU film significantly increased upon visible-light exposure (Fig. 3c), and the surface temperature of the elongated 5CAZ/5CB/GO(3wt‰)/SMPU film rose to 45.1 °C in the process of visible-light exposure (Fig. 3d), 5.6 °C higher than the T_i (39.5 °C) of the LC mixture, demonstrating that the visible light-induced bending deformation of the elongated 5CAZ/5CB/GO(3wt‰)/SMPU film is ascribed to a combination of the photochemically triggered LC-to-I phase transition caused by the *trans*-to-*cis* photoisomerization of 5CAZ and the photothermally induced LC-to-I phase transition derived from the photothermal effect of GO. Upon NIR (808 nm, 210 mW/cm^2) exposure, the elongated SMPU, 5CB/SMPU and 5CAZ/5CB/SMPU films were unbending due to the absence of GO (Fig. 3e). When GO was incorporated into the SMPU film, the elongated GO/SMPU film showed a large F value of 0.30 upon NIR irradiation (Fig. 3e), which was because the photothermal effect of GO enabled the surface temperature of the composite film to rise to 72.1 °C in the process of NIR exposure (Fig. 3f), much higher than the T_gh of SMPU (53.5 °C), leading to the partial stress relaxation of the composite film.[40] When the elongated 5CAZ/5CB/GO(3wt‰)/SMPU film was exposed to NIR light (808 nm, 210 mW/cm^2), it showed a larger F value (F=0.51) than the GO/SMPU film (Fig. 3e), which was because the photothermal effect of GO enabled the surface temperature of the composite film to reach 67.6 °C in the process of NIR irradiation (Fig. 3f), much higher than the T_i (39.5 °C) of the LC mixture and the T_gh of SMPU (53.5 °C), leading to a combination of the photothermally induced LC-to-I phase transition and the partial stress relaxation of the composite film.

As is well-known, the shape-memory property is considered to be an important factor in determining the performances of SMPMs, which is of great significance to the practical applications of SMPMs.[41–43] The sequential shape changes of the 5CAZ/5CB/GO(3wt‰)/SMPU film is shown in Fig. 4(a). Firstly, the composite film was stretched to 200% strain by using a universal testing machine at 65 °C, followed by cooling to room temperature slowly to obtain the elongated temporary shape (shape fixing ratio R_f=70.0%±2.3%). Subsequently, the elongated composite film was upswept by exposure to UV light (365 nm, 110 mW/cm^2) for 100 s, visible light (460 nm, 110 mW/cm^2) for 108 s or NIR light (808 nm, 210 mW/cm^2) for 65 s, which could nearly revert to its original flat shape (shape recovery ratio R_r=88.3%±3.5%) upon high-intensity NIR (808 nm, 470 mW/cm^2) exposure (Movie S10 in ESI) because the photothermal effect of GO enabled the upper and lower surface temperatures of the composite film to rise to be above 80 °C (Fig. 4b), much higher than the

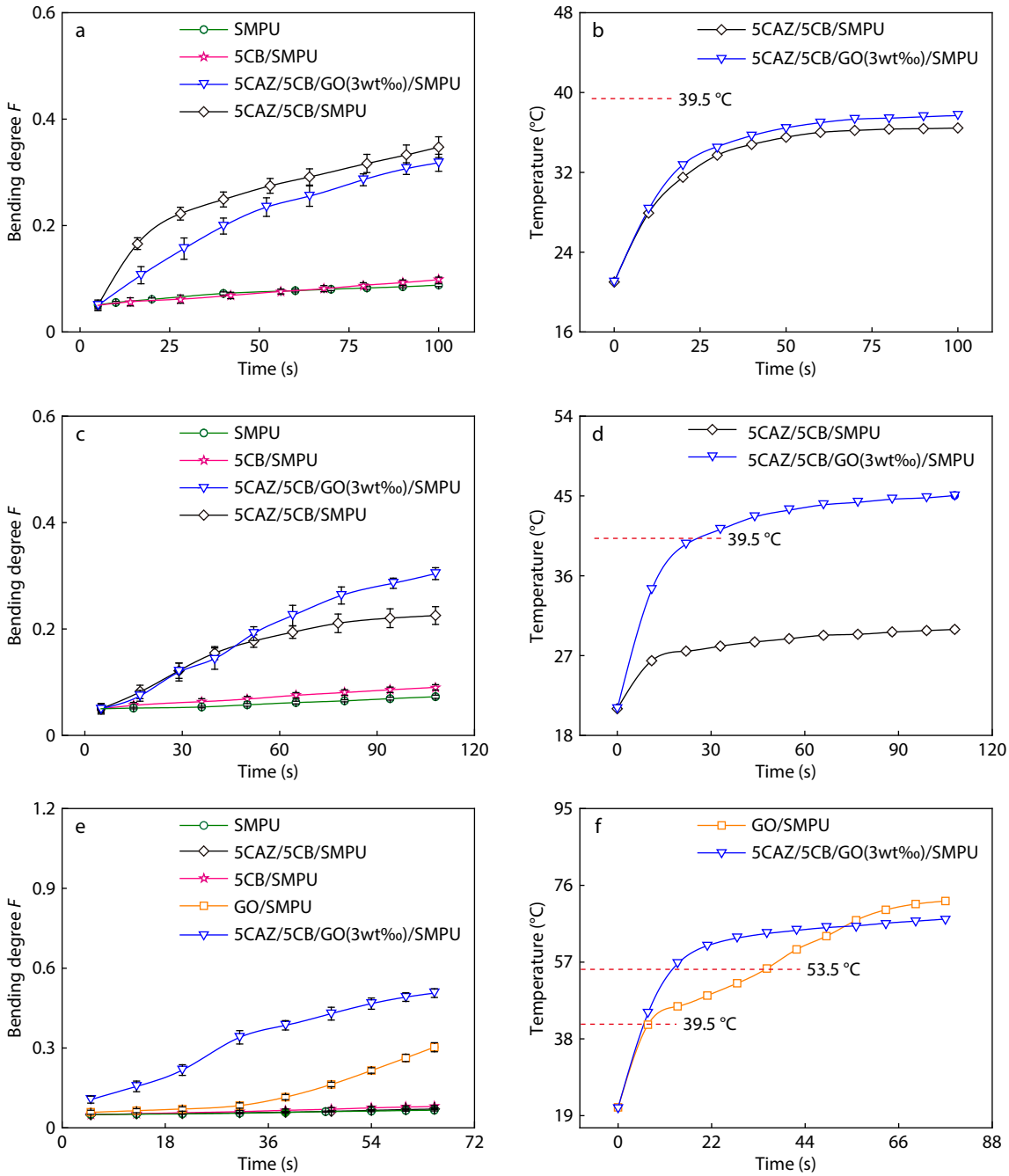

Fig. 3 (a) Changes in the bending degrees of four films with time upon UV (365 nm, 110 mW/cm^2) irradiation; (b) Changes in the surface temperatures of two films with time upon UV (365 nm, 110 mW/cm^2) exposure; (c) Changes in the bending degrees of four films with time upon visible-light (460 nm, 110 mW/cm^2) irradiation; (d) Changes in the surface temperatures of two films with time upon visible-light (460 nm, 110 mW/cm^2) exposure; (e) Changes in the bending degrees of five films with time upon NIR (808 nm, 210 mW/cm^2) irradiation; (f) Changes in the surface temperatures of two films with time upon NIR (808 nm, 210 mW/cm^2) exposure.

T_gh of SMPU (53.5 °C), thereby leading to the sufficient stress relaxation of the composite film.[40] It is worth noting that the sequential shape changes of the 5CAZ/5CB/GO(3wt‰)/SMPU film could be reversibly achieved upon sequential thermal stretching and light irradiation.

Application: Biomimetic Actuators

Currently, inspired by natural movements, the biomimetic researches are in full swing, and the excellent light-deformations of the composite film enables it more advantageous in the field of biomimetic functional devices. By means of the light-induced sequential shape changes of the 5CAZ/5CB/GO(3wt‰)/SMPU film, the biomimetic circadian rhythms of acacia leaves (the opening and closing of leaves) were successfully achieved. Firstly, four composite films with dimensions of 5 mm (length) × 5 mm (width) × 0.3 mm (thickness) were stretched to 200% strains at 65 °C, and then

the four elongated films bonded with green rectangular cardboards were glued to a plastic rod by using the double-sided adhesive. As shown in Fig. 5(a), upon UV (365 nm, 110 mW/cm^2), visible (460 nm, 110 mW/cm^2) or NIR (808 nm, 210 mW/cm^2) exposure, the elongated composite films bent towards the light source, simulating the closing of acacia leaves (Movie S11 in ESI). Upon high-intensity NIR (808 nm, 470 mW/cm^2) irradiation, the bent composite films almost returned to their original flat shapes, mimicking the opening of acacia leaves. In addition, the biomimetic bending/spreading of fingers were also successfully achieved by utilizing the 5CAZ/5CB/GO(3wt‰)/SMPU films. Firstly, black elongated composite films with 200% strains were glued to a yellow rectangular 5CAZ/SMPU film by using DMF. As shown in

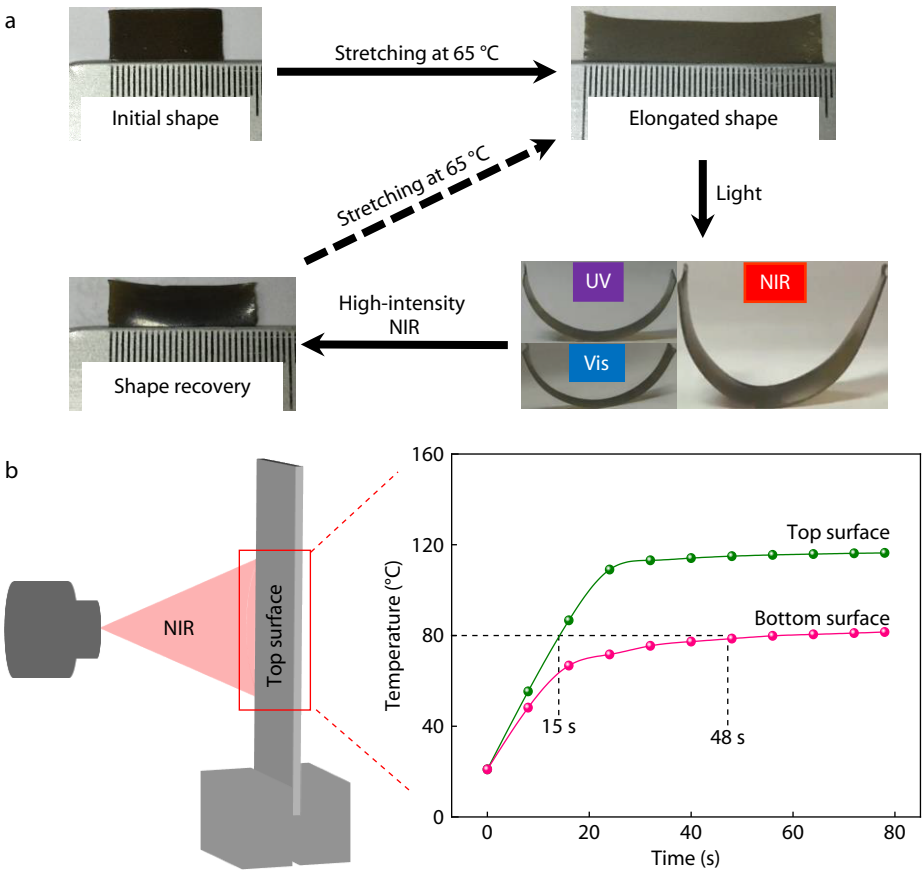

Fig. 4 (a) Photographs showing the sequential shape changes of the composite films. The elongated composite films were exposed to UV (365 nm, 110 mW/cm^2) for 100 s, Vis light (460 nm, 110 mW/cm^2) for 108 s and NIR light (808 nm, 210 mW/cm^2) for 65 s; (b) Changes in the upper and lower surface temperatures of the composite film with time upon high-intensity NIR (808 nm, 470 mW/cm^2) exposure.

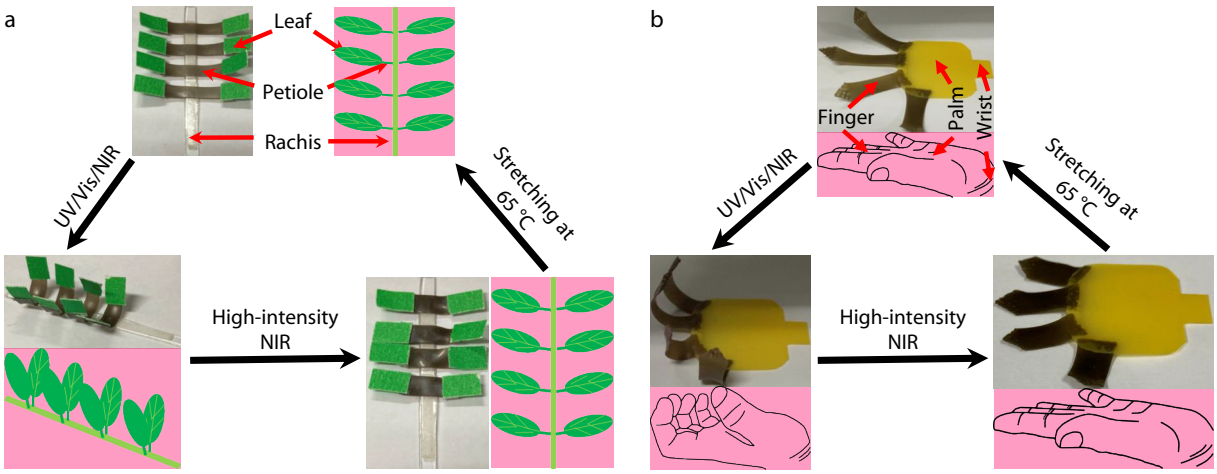

Fig. 5 (a) Photographs showing the biomimetic circadian rhythms of acacia leaves; (b) Photographs exhibiting the biomimetic bending/spreading of fingers.

https://doi.org/10.1007/s10118-022-2657-9

Fig. 5(b), when exposed to UV (365 nm, 110 mW/cm^2), visible (460 nm, 110 mW/cm^2) or NIR (808 nm, 210 mW/cm^2) light, the black composite films bent towards the incident direction of the actinic light, simulating the bending of fingers (Movie S12 in ESI). Upon high-intensity NIR (808 nm, 470 mW/cm^2) exposure, the bent composite films nearly reverted to their original flat shapes, mimicking the spreading of fingers. Moreover, it is worth noting that the biomimetic circadian rhythms of acacia leaves and the biomimetic bending/spreading of fingers could be reversibly achieved upon successive thermal stretching and photoirradiation.

CONCLUSIONS

In summary, a UV-Vis-NIR light-deformable SMPU-based composite film was successfully prepared. Due to the surface migrations of 5CAZ and 5CB in the film-forming process, the composite film spontaneously formed a bilayer-like structure with the upper part as a LC-rich layer and the lower part as a LC-poor one. The elongated composite films not only showed UV-induced bending deformations triggered by the photochemically induced LC phase transition, but also exhibited visible light-triggered bending deformations attributed to the photochemically and photothermally induced LC phase transition, and NIR-induced bending deformations caused by the photothermally triggered LC phase transition and the partial stress relaxation of the composite films. By introducing the photothermal effect, the bending degrees and bending speeds of the composite films were improved. All the deformations were capable of shape recoveries by exposure to high-intensity NIR light. It is worth mentioning that the sequential shape changes of the composite film could be reversibly achieved upon sequential thermal stretching and photoirradiation. Attractively, by means of the light-induced sequential shape changes of the composite film, the biomimetic circadian rhythms of acacia leaves and the biomimetic bending/spreading of fingers were successfully and reversibly achieved, which could be promising in the field of biomimetic functional devices. The UV-Vis-NIR light-deformable composite could be promising for the utilization of solar energy, and might be used as a sunlight-driven functional material in the near future.

NOTES

The authors declare no competing financial interest.

Electronic Supplementary Information

Electronic supplementary information (ESI) is available free of charge in the online version of this article at http://doi.org/10.1007/s10118-022-2657-9.

ACKNOWLEDGMENTS

This work was financially supported by the National Natural Science Foundation of China (Nos. 51373025, 51773002 and 51921002).

REFERENCES

1 Yu, H.; Ikeda, T. Photocontrollable liquid-crystalline actuators. *Adv. Mater.* **2011**, *23*, 2149–2180.
2 Zhao, Q.; Qi, H. J.; Xie, T. Recent progress in shape memory polymer: new behavior, enabling materials, and mechanistic understanding. *Prog. Polym. Sci.* **2015**, *49–50*, 79–120.
3 Song, L.; Li, Y.; Xiong, Z.; Pan, L.; Luo, Q.; Xu, X.; Lu, S. Water-induced shape memory effect of nanocellulose papers from sisal cellulose nanofibers with graphene oxide. *Carbohyd. Polym.* **2018**, *179*, 110–117.
4 Zhang, Y.; Zhang, M.; Jiang, H.; Shi, J.; Li, F.; Xia, Y.; Zhang, G.; Li, H. Bio-inspired layered chitosan/graphene oxide nanocomposite hydrogels with high strength and pH-driven shape memory effect. *Carbohyd. Polym.* **2017**, *177*, 116–125.
5 Park, J. K.; Nan, K.; Luan, H.; Zheng, N.; Zhao, S.; Zhang, H.; Cheng, X.; Wang, H.; Li, K.; Xie, T.; Huang, Y.; Zhang, Y.; Kim, S.; Rogers, J. A. Remotely triggered assembly of 3D mesostructures through shape-memory effects. *Adv. Mater.* **2019**, *31*, 1905715.
6 Rehman, H. U.; Chen, Y.; Hedenqvist, M. S.; Li, H.; Xue, W.; Guo, Y.; Guo, Y.; Duan, H.; Liu, H. Self-healing shape memory PUPCL copolymer with high cycle life. *Adv. Funct. Mater.* **2017**, *28*, 1704109.
7 Peng, K.; Zhao, Y.; Shahab, S.; Mirzaeifar, R. Ductile shape-memory polymer composite with enhanced shape recovery ability. *ACS Appl. Mater. Interfaces* **2020**, *12*, 58295–58300.
8 Xie, T. Tunable polymer multi-shape memory effect. *Nature* **2010**, *464*, 267–270.
9 Bellin, I.; Kelch, S.; Langer, R.; Lendlein, A. Polymeric triple-shape materials. *Proc. Natl. Acad. Sci. USA* **2006**, *103*, 18043–18047.
10 Wang, X.; Lan, J.; Wu, P.; Zhang, J. Liquid metal based electrical driven shape memory polymers. *Polymer* **2021**, *212*, 112174.
11 Wang, W.; Liu, D.; Liu, Y.; Leng, J.; Bhattacharyya, D. Electrical actuation properties of reduced graphene oxide paper/epoxy-based shape memory composites. *Compos. Sci. Technol.* **2015**, *106*, 20–24.
12 Chen, Y.; Zhao, X.; Li, Y.; Jin, Z.; Yang, Y.; Yang, M.; Yin, B. Light- and magnetic-responsive synergy controlled reconfiguration of polymer nanocomposites with shape memory assisted self-healing performance for soft robotics. *J. Mater. Chem. C* **2021**, *9*, 5515–5527.
13 Liu, J. A. C.; Evans, B. A.; Tracy, J. B. Photothermally reconfigurable shape memory magnetic cilia. *Adv. Mater. Technol.* **2020**, *5*, 2000147.
14 Xiao, Y.; Gong, X.; Kang, Y.; Jiang, Z.; Zhang, S.; Li, B. Light-, pH- and thermal-responsive hydrogels with the triple-shape memory effect. *Chem. Commun.* **2016**, *52*, 10609–10612.
15 Sessini, V.; Arrieta, M P.; Fernández-Torres, A.; Peponi, L. Humidity-activated shape memory effect on plasticized starch-based biomaterials. *Carbohyd. Polym.* **2018**, *179*, 93–99.
16 Huang, Y.; Bisoyi, H. K.; Huang, S.; Wang, M.; Chen, X.; Liu, Z.; Yang, H.; Li, Q. Bioinspired synergistic photochromic luminescence and programmable liquid crystal actuators. *Angew. Chem. Int. Ed.* **2021**, *60*, 11247–11251.
17 Zheng, Z.; Li, Y.; Bisoyi, H. K.; Wang, L.; Bunning, T. J.; Li, Q. Three-dimensional control of the helical axis of a chiral nematic liquid crystal by light. *Nature* **2016**, *531*, 352–356.
18 Li, G.; Zhang, H.; Fortin, D.; Fan, W.; Xia, H.; Zhao, Y. A composite material with room temperature shape processability and optical repair. *J. Mater. Chem. C* **2016**, *4*, 5932–5939.
19 Yang, L.; Wang, Z.; Fei, G.; Xia, H. Polydopamine particles reinforced poly(vinyl alcohol) hydrogel with NIR light triggered shape memory and self-healing capability. *Macromol. Rapid Commun.* **2017**, *38*, 1700421.
20 Zhang, P.; Cai, F.; Wang, W.; Wang, G.; Yu, H. Light-switchable

adhesion of azobenzene-containing siloxane-based tough adhesive. *ACS Appl. Polym. Mater.* **2021**, *3*, 2325–2329.
21 Yu, H. Recent advances in photoresponsive liquid-crystalline polymers containing azobenzene chromophores. *J. Mater. Chem. C* **2014**, *2*, 3047–3054.
22 Qin, L.; Liu, X.; Yu, Y. Soft actuators of liquid crystal polymers fueled by light from ultraviolet to near infrared. *Adv. Opt. Mater.* **2021**, *9*, 2001743.
23 Hu, J.; Li, X.; Ni, Y.; Ma, S.; Yu, H. A programmable and biomimetic photo-actuator: a composite of a photo-liquefiable azobenzene derivative and commercial plastic film. *J. Mater. Chem. C* **2018**, *6*, 10815–10821.
24 Li, X.; Ma, S.; Hu, J.; Ni, Y.; Lin, Z.; Yu, H. Photo-activated bimorph composites of Kapton and liquid-crystalline polymer towards biomimetic circadian rhythms of *Albizia julibrissin* leaves. *J. Mater. Chem. C* **2019**, *7*, 622–629.
25 Liu, X.; Wang, X. Recent progresses in side-on liquid crystalline elastomers. *Acta Polymerica Sinica* (in Chinese) **2017**, 1549–1556.
26 Wang, J.; Huang, S.; Zhang, Y.; Liu, J.; Yu, M.; Yu, H. Hydrogen bond enhances photomechanical swing of liquid-crystalline polymer bilayer films. *ACS Appl. Mater. Interfaces* **2021**, *13*, 6585–6596.
27 Pang, X.; Xu, B.; Qing, X.; Wei, J.; Yu, Y. Photo-induced bending behavior of post-crosslinked liquid crystalline polymer/polyurethane blend films. *Macromol. Rapid Commun.* **2018**, *39*, 1700237.
28 Fang, T.; Cao, L.; Chen, S.; Fang, J.; Zhou, J.; Fang, L.; Lu, C.; Xu, Z. Preparation and assembly of five photoresponsive polymers to achieve complex light-induced shape deformations. *Mater. Design* **2018**, *144*, 129–139.
29 Weis, P.; Wu, S. Light-switchable azobenzene-containing macromolecules: from UV to near infrared. *Macromol. Rapid Commun.* **2018**, *39*, 1700220.
30 Wu, S.; Butt, H. J. Near-infrared-sensitive materials based on upconverting nanoparticles. *Adv. Mater.* **2016**, *28*, 1208–1226.
31 Cheng, Z.; Wang, T.; Li, X.; Zhang, Y.; Yu, H. NIR-Vis-UV light-responsive actuator films of polymer-dispersed liquid crystal/graphene oxide nanocomposites. *ACS Appl. Mater. Interfaces* **2015**, *7*, 27494–27501.
32 Zhang, P.; Wu, B.; Huang, S.; Cai, F.; Wang, G.; Yu, H. UV-Vis-NIR light-induced bending of shape-memory polyurethane composites doped with azobenzene and upconversion nanoparticles. *Polymer* **2019**, *178*, 121644.
33 Zhou, L.; Liu, Q.; Lv, X.; Gao, L.; Fang, S.; Yu, H. Photoinduced triple shape memory polyurethane enabled by doping with azobenzene and GO. *J. Mater. Chem. C* **2016**, *4*, 9993–9997.
34 Kim, B. K.; Lee, S. Y. Polyurethanes having shape memory effects. *Polymer* **1996**, *37*, 5781–5793.
35 Li, F.; Hou, J.; Zhu, W.; Zhang, X.; Xu, M.; Luo, X.; Ma, D.; Kim, B. K. Crystallinity and morphology of segmented polyurethanes with different soft-segment length. *J. Appl. Polym. Sci.* **1996**, *62*, 631–638.
36 Yun, X.; Tang, B.; Xiong, Z.; Wang, X. Understanding self-assembly, colloidal behavior and rheological properties of graphene derivatives for high-performance supercapacitor fabrication. *Chinese J. Polym. Sci.* **2020**, *38*, 423–434.
37 Yu, L.; Cheng, Z.; Dong, Z.; Zhang, Y.; Yu, H. Photomechanical response of polymer-dispersed liquid crystals/graphene oxide nanocomposites. *J. Mater. Chem. C* **2014**, *2*, 8501–8506.
38 Qing, X.; Qin, L.; Gu, W.; Yu, Y. Deformation of cross-linked liquid crystal polymers by light-from ultraviolet to visible and infrared. *Liq. Cryst.* **2016**, *43*, 2114–2135.
39 Ube, T.; Takado, K.; Ikeda, T. Photomobile materials with interpenetrating polymer networks composed of liquid-crystalline and amorphous polymers. *J. Mater. Chem. C* **2015**, *3*, 8006–8009.
40 Wang, W.; Lu, H.; Liu, Y.; Leng, J. Sodium dodecyl sulfate/epoxy composite: water-induced shape memory effect and its mechanism. *J. Mater. Chem. A* **2014**, *2*, 5441–5449.
41 Meng, H.; Li, G. A review of stimuli-responsive shape memory polymer composites. *Polymer* **2013**, *54*, 2199–2221.
42 Delaey, J.; Dubruel, P.; Vlierberghe, S. V. Shape-memory polymers for biomedical applications. *Adv. Funct. Mater.* **2020**, *30*, 1909047.
43 Hu, J.; Zhu, Y.; Huang, H.; Lu, J. Recent advances in shape-memory polymers: structure, mechanism, functionality, modeling and applications. *Prog. Polym. Sci.* **2012**, *37*, 1720–1763.

https://doi.org/10.1007/s10118-022-2657-9